Available online at www.sciencedirect.com

ScienceDirect

Procedia Structural Integrity 2 (2016) 3109–3116

Structural Integrity Procedia

www.elsevier.com/locate/procedia

21st European Conference on Fracture, ECF21, 20-24 June 2016, Catania, Italy

Biaxial Experiments and Numerical Simulations on Damage and Fracture Mechanisms in Ductile Metals at Different Loading Conditions

Michael Brünig[a,*], Steffen Gerke[a], Marco Schmidt[a]

[a]*Institut für Mechanik und Statik, Universität der Bundeswehr München, Werner-Heisenberg-Weg 39, 85577 Neubiberg, Germany*

Abstract

The paper deals with an anisotropic damage and fracture model for ductile metals. The phenomenological approach takes into account the effect of stress state on damage condition and damage strain evolution laws. Different branches of these criteria are considered corresponding to different damage and fracture mechanisms depending on stress triaxiality and the Lode parameter. To validate these criteria new experiments with two-dimensionally loaded specimens are presented. Specimen's geometry and loading conditions as well as their influence on stress states are discussed in detail. They allow combined shear-tension and shear-compression stress states. Digital image correlation technique has been used to analyze current strain fields in critical regions of the specimens. Corresponding numerical simulations of the experiments show that they cover a wide range of stress states.

Peer-review under responsibility of the Scientific Committee of ECF21.

Keywords: Experiments; Digital image correlation technique; Numerical simulations; Stress state dependence; Ductile damage and fracture

1. Introduction

During the last decades the demand for and the use of high quality metals like high strength steels, advanced high strength steels and aluminum alloys has been remarkably increased. For example, there are requirements on lightweight design leading to improved energy consumption or cost efficiency and, at the same time, to enforce the safety demands. Therefore, material properties have to be enhanced to avoid early localization of inelastic strains as well as damage and fracture of structural components undergoing complex loading conditions. In this context, advanced constitutive models are needed to simulate the material behavior under different loading processes.

Based on intensive experimental and numerical investigations it is now well known that the characteristics of damage and fracture mechanisms depend on stress state acting in a material point. For example, under tension loading conditions with high positive stress triaxialities damage in ductile metals is mainly caused by nucleation, growth and coalescence of micro-voids. On the other hand, under shear and compression loading conditions with nearly zero or negative stress triaxiality the predominant damage mechanisms are formation, growth and coalescence of micro-

* Corresponding author. Tel.: +49-89-60043415 ; fax: +49-89-60044549.
E-mail address: michael.bruenig@unibw.de

Peer-review under responsibility of the Scientific Committee of ECF21.
10.1016/j.prostr.2016.06.388

shear-cracks. Furthermore, for moderate positive stress triaxialities combination of these basic microscopic damage processes occurs whereas no damage has been observed in ductile metals for high negative stress triaxialities. Hence, ductile damage behavior and crack formation strongly depend on the stress state. This has to be taken into account in development of accurate and realistic phenomenological continuum damage and fracture models which must be based on detailed experimental investigations and corresponding numerical simulations.

Various experiments with carefully designed metal specimens have been proposed in the literature. For example, uniaxial tension tests with un-notched and pre-notched specimens and corresponding numerical simulations have been performed by Bao and Wierzbicki (2004); Brünig et al (2008); Gao et al (2010); Dunand and Mohr (2011) to study the dependence of damage and failure on positive stress triaxialities. To investigate the damage and fracture behavior under nearly zero stress triaxialities where shear mechanisms occur in the critical parts of the specimens new geometries of uniaxially loaded specimens have been developed and tested by Bao and Wierzbicki (2004); Brünig et al (2008); Gao et al (2010); Driemeier et al (2010). In addition, butterfly specimens with complex geometries have been proposed by Bai and Wierzbicki (2008); Dunand and Mohr (2011) to analyze the behavior under positive and negative stress triaxialities. The specimens are loaded in uniaxial experiments in different directions using special testing equipment. Alternatively, biaxial experiments with new shear-tension-specimens have been developed by Brünig et al (2015, 2016) to investigate stress-state-dependent damage and fracture processes. Corresponding numerical simulations have shown that their tests cover a wide range of positive and negative stress triaxialities. Additional scanning electron microscope analyses of fracture surfaces have elucidated different mechanisms of ductile fracture on the micro-level.

In the present paper a phenomenological continuum damage model will be briefly discussed. Experiments with biaxially loaded specimens will be presented here with focus on the region of negative stress triaxialities. In critical regions of the specimens evolution of strain fields is analyzed by digital image correlation. Corresponding numerical simulations have been performed and numerical results will be used to explain stress-state-dependent damage and fracture mechanisms especially for shear-compression loading conditions.

2. Continuum damage model

The anisotropic continuum damage model proposed by Brünig (2003); Brünig et al (2015) is used to predict evolution of damage and fracture in ductile metals. The phenomenological approach is based on the kinematic model with additive decomposition of the strain rate tensor into elastic, plastic and damage parts. Free energy functions with respect to undamaged and damaged configurations are introduced. They lead to respective elastic laws which in the damaged configurations are affected by increasing damage to simulate deterioration of elastic material properties caused by growth of micro-defects. Considering the undamaged configurations plastic behavior is modeled by a yield condition and a flow rule. In a similar way, damage behavior is governed by a damage condition and a damage rule, both formulated with respect to the damaged configurations.

In particular, determination of onset and continuation of damage is based on the concept of a damage surface formulated in stress space. Thus, the damage condition

$$f^{da} = \alpha I_1 + \beta \sqrt{J_2} - \sigma = 0 \tag{1}$$

is expressed in terms of the first and second deviatoric stress invariants, I_1 and J_2, of the Kirchhoff stress tensor and the damage threshold σ represents the material toughness to micro-defect propagation. In Eq. (1) the variables α and β are damage mode parameters corresponding to the different damage mechanisms acting on the micro-level: shear modes for negative stress triaxialities, void-growth-dominated modes for large positive triaxialities and mixed modes (simultaneous growth of micro-voids and evolution of micro-shear-cracks) for lower positive stress triaxialities. These damage mode parameters α and β depend on the stress triaxiality

$$\eta = \frac{\sigma_m}{\sigma_{eq}} = \frac{I_1}{3\sqrt{3J_2}} \tag{2}$$

defined as the ratio of the mean stress $\sigma_m = I_1/3$ and the von Mises equivalent stress $\sigma_{eq} = \sqrt{3J_2}$ as well as on the Lode parameter

$$\omega = \frac{2T_2 - T_1 - T_3}{T_1 - T_3} \quad \text{with } T_1 \geq T_2 \geq T_3 \tag{3}$$

expressed in terms of the principal Kirchhoff stress components T_1, T_2 and T_3.

For the investigated aluminum alloy the dependence of α and β on stress state has been investigated by Brünig et al (2013). They performed micro-mechanical calculations considering deformation behavior of micro-defects in differently 3D-loaded void-containing unit cells. Based on their numerical results and numerical simulations of biaxial experiments performed by Brünig et al (2015, 2016), the parameter α is taken to be

$$\alpha(\eta) = \begin{cases} -0.15 \;\; \text{for} \;\; \eta_{cut} < \eta \leq 0 \\ 0.33 \;\; \text{for} \;\; \eta > 0 \end{cases} \tag{4}$$

where η_{cut} represents the cut-off value of the stress triaxiality below which damage and fracture will not occur. In addition, the parameter β is given by the non-negative function

$$\beta(\eta,\, \omega) = \beta_0(\eta,\, \omega = 0) + \beta_\omega(\omega) \geq 0 \;, \tag{5}$$

with

$$\beta_0(\eta) = -1.28\,\eta + 0.85 \tag{6}$$

and

$$\beta_\omega(\omega) = -0.017\,\omega^3 - 0.065\,\omega^2 - 0.078\,\omega \;. \tag{7}$$

Furthermore, the damage strain rate tensor is given by the damage rule

$$\dot{\mathbf{H}}^{da} \;=\; \dot{\mu}\, \left(\bar{\alpha}\, \frac{1}{\sqrt{3}}\, \mathbf{1} + \bar{\beta}\, \mathbf{N} + \bar{\delta}\, \mathbf{M} \right) \tag{8}$$

where the normalized stress related deviatoric tensors $\mathbf{N} = \frac{1}{2\sqrt{J_2}}\, \text{dev}\tilde{\mathbf{T}}$ and $\mathbf{M} = \frac{1}{\|\text{dev}\tilde{\mathbf{S}}\|}\, \text{dev}\tilde{\mathbf{S}}$ with the quadratic function of the stress deviator

$$\text{dev}\tilde{\mathbf{S}} = \text{dev}\tilde{\mathbf{T}}\; \text{dev}\tilde{\mathbf{T}} - \frac{2}{3}\; J_2\; \mathbf{1} \tag{9}$$

have been used. In Eq. (8) $\dot{\mu}$ represents in the proposed continuum damage model the equivalent damage strain rate measure characterizing the amount of increase in irreversible damage strains. The parameters $\bar{\alpha}$, $\bar{\beta}$ and $\bar{\delta}$ are kinematic variables describing the portion of volumetric and isochoric damage-based deformations. In particular, the parameter $\bar{\alpha}$ characterizes the amount of volumetric damage strain rates caused by isotropic volume change of micro-defects and is given by

$$\bar{\alpha}(\eta) = \begin{cases} 0 \;\; \text{for} \;\; \eta_{cut} < \eta \leq 0 \\ 0.5714\,\eta \;\; \text{for} \;\; 0 < \eta \leq 1.75 \\ 1 \;\; \text{for} \;\; \eta > 1.75 \end{cases} \;. \tag{10}$$

The parameter $\bar{\beta}$ corresponds to the amount of anisotropic isochoric damage strain rates caused by evolution of micro-shear-cracks and is taken to be

$$\bar{\beta}(\eta,\, \omega) = \bar{\beta}_0(\eta) + f_\beta(\eta)\, \bar{\beta}_\omega(\omega) \tag{11}$$

with

$$\bar{\beta}_0(\eta) = \begin{cases} 0.87 \;\; \text{for} \;\; \eta_{cut} < \eta \leq \frac{1}{3} \\ 0.97875 - 0.32625\,\eta \;\; \text{for} \;\; \frac{1}{3} < \eta \leq 3 \\ 0 \;\; \text{for} \;\; \eta > 3 \end{cases} \;, \tag{12}$$

$$f_\beta(\eta) = -0.0252 + 0.0378\,\eta \tag{13}$$

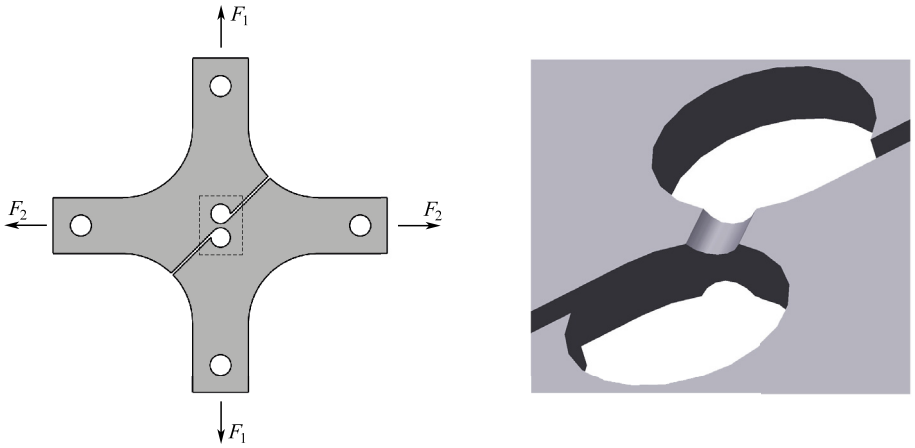

Fig. 1. (a) Specimen and loading conditions; (b) Detail of the notched central part.

and

$$\bar{\beta}_{\omega}(\omega) = \begin{cases} 1-\omega^2 \ \text{ for } \ \eta_{cut} < \eta \leq \frac{2}{3} \\ 0 \ \text{ for } \ \eta > \frac{2}{3} \end{cases} . \tag{14}$$

Based on numerical simulations of biaxial experiments with different stress triaxialities performed by Brünig et al (2016) the parameter $\bar{\delta}$ is taken to be zero in the present investigation.

It should be noted that the macroscopic damage rule (8) applicable for different loading conditions is based on the introduction of micro-structurally based damage variables which not only represent the volume fraction of the micro-defects but also take into account their current shape and orientation. For example, it takes into account volumetric parts (first term in Eq. (8)) corresponding to isotropic growth of voids on the micro-scale as well as deviatoric parts (second and third term in Eq. (8)) associated with anisotropic evolution of micro-shear-cracks, respectively. Therefore, both basic damage mechanisms discussed above (growth of isotropic micro-voids and evolution of micro-shear-cracks) acting on the micro-level are involved in the macroscopic damage rule (8) of the phenomenological continuum model.

3. Experiments and numerical simulations

A new experimental program has been developed to propose new tests to study the effect of stress state on inelastic behavior, damage and fracture in ductile metals. The experiments are performed using a biaxial testing machine containing four electro-mechanically driven cylinders with load maxima of 20kN.

The material under investigation is an aluminum alloy of series 2017. Geometry and loading conditions of the specimens are shown in Fig. 1. In the center of the specimen additional notches in thickness direction have been milled leading to localization of inelastic deformations, damage and fracture in this part which is 3mm high with thickness of 2mm and the radius of the notch is 2mm. During the tests the specimens are simultaneously loaded in vertical and in horizontal direction by the forces F_1 and F_2. The vertical load F_1 leads to shear mechanisms in the center of the specimen whereas the load F_2 leads in this part to superimposed tension or compression modes.

To analyze in the experimental program in detail the deformation behavior in the critical zones of the specimens digital image correlation (DIC) technique has been applied. The three-dimensional displacement field of the specimen surface was taken by two cameras and evaluated by the digital image correlation system provided by Dantec/Limess. Specimen preparation was realized shortly before the experiment started. One side of the specimen was firstly sprayed with a white acrylic lacquer and then the speckle pattern shown in Fig. 2 was sprayed on with a black acrylic lacquer using an air brush system to achieve a sufficiently fine pattern. Specimen preparation was realized shortly before the experiment was performed to avoid excessive curing and, thus, no ex-foliation of the coating was observed during the

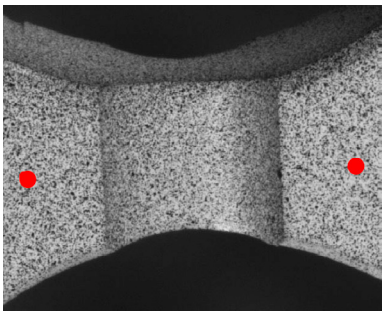

Fig. 2. Speckle pattern of the specimen's center incl. emphasis of points (red) for displacement measurements.

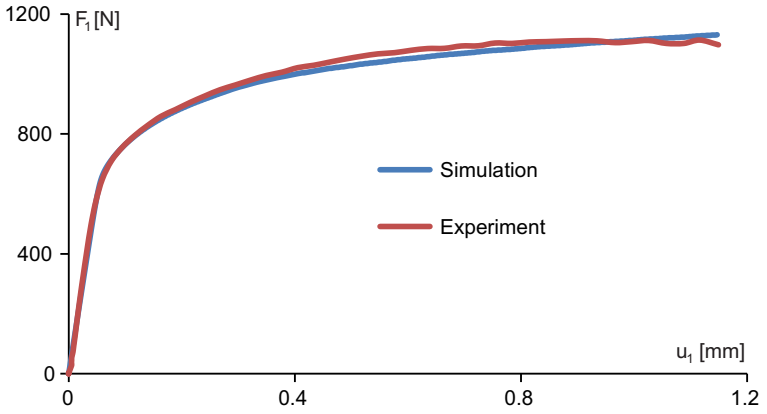

Fig. 3. Load-displacement curves $F_1 - u_1$.

tests. The displacements correspond to movements of the selected points marked in red in Fig. 2. For example, the vertical displacement u_1 is the vertical relative movement of these points whereas the displacement u_2 is the horizontal one. In addition, the corresponding forces in axes directions were transferred and stored with the data sets of the image correlation system at a frequency of 0.25Hz while the velocity of the machine was 0.04mm/min.

Furthermore, numerical simulations of the experiments have been performed. They deliver detailed information on distributions and amount of stresses and strains especially in the critical regions of the specimens. The numerical calculations are carried out using the finite element program ANSYS enhanced by a user-defined material subroutine based on the continuum model discussed above. Numerical results are compared with available experimental data to analyze localized deformation and failure behavior.

In the present paper, results of experiments and of corresponding numerical simulations are shown for the shear-compression range with the load ratio $F_1 : F_2 = 1 : -2$. The load-displacement curves $F_1 - u_1$ are shown in Fig. 3. A large region with inelastic behavior including hardening is observed after elastic loading. The load maximum is about $F_1 = 1100N$ and final fracture of the specimen occurred at $u_1 = 1.15mm$. The numerically predicted curve shows very good agreement with the experimental one.

Furthermore, damage and fracture behavior is analyzed in critical regions of the specimen where inelastic deformations are localized and final fracture occurred in the experiments. In particular, numerically predicted fields of stress triaxialities η and of the Lode parameter ω in a vertical cut in the specimen's center at the end of the loading process are shown in Fig. 4. For the investigated load ratio $F_1 : F_2 = 1 : -2$ the stress triaxiality is numerically predicted to be here nearly constant with $\eta = -0.3$ and only in the upper and lower boundaries positive stress triaxialities can be seen. In addition, the Lode parameter is about $\omega = -0.2$ in the center and reaches $\omega = -1.0$ at the boundaries. For these stress parameters damage will be mainly caused by formation and growth of micro-shear-cracks whereas the effect of micro-voids will be marginal which is characteristic for shear-compression loading conditions.

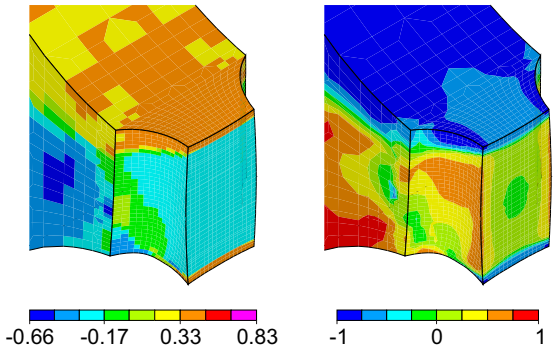

Fig. 4. Stress triaxiality η (left) and Lode parameter ω (right).

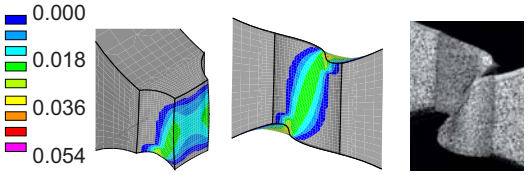

Fig. 5. Equivalent damage strain μ and experimental fracture line.

The equivalent damage strain μ, see Eq. (8), is used to quantify the amount of damage strains. Figure 5 shows its numerically predicted distribution in the notched part of the specimen shortly before fracture occurred in the experiments. The equivalent damage strain μ has its maxima of about $\mu = 4.5\%$ at the boundaries of the notch but is also of about $\mu = 2.5\%$ in the band between these points. These damage strain quantities are predicted only to occur in this band and, therefore, onset of macro-cracking is expected to be initiated in this part of the specimen. The crack will then run along the band of moderate equivalent damage strains where are the weakest points of the material. This band of damage strains nicely corresponds to the fracture line of the tested specimen also shown in Fig. 5. In addition, the geometry of the deformed specimen predicted by the numerical calculation agrees very well with the geometry of the tested specimen shown in the picture.

Figure 6 shows comparison of strain fields of the tested specimens analyzed by DIC in the load step shortly before final fracture occurs with corresponding fields predicted by numerical simulations based on the continuum model discussed above. In particular, in Fig. 6(a) the distribution of the normal strain component in direction 1 (see Fig. 1) is visualized, the normal strain component in direction 2 is shown in Fig. 6(b) and the distribution of the shear strain can be seen in Fig. 6(c). For example, the normal strain component in direction 1 analyzed by DIC during the experiment (top picture in Fig. 6(a)) is characterized by a localized band with maximum values of about 17%. This normal strain distribution agrees well with that one predicted by the numerical simulation shown in the bottom picture in Fig. 6(a) and the numerical values are slightly larger (about 20%). The distribution of the normal strain component in direction 2 taken from DIC and that one obtained from numerical simulation are shown in Fig. 6(b) which also show good agreement. A similar localized band of this normal strain component can be seen with minimum values of about -23% in the experiment caused by the superimposed compression load and, again, numerically predicted values are slightly larger (about -26%). In addition, distributions of the shear strain are shown in Fig. 6(c). Experimental values analyzed by DIC (top picture) are also localized in a small band with values up to about 42%. Corresponding shear strains based on numerical analysis (bottom picture) show similar distribution but with maxima of only about 33%. A reason for this difference in strain components may be the possible early occurrence of shear-cracks in this band. Their effect can also be seen in the experimental load-displacement curves (Fig. 3) where small waves appear before final fracture. Thus, further softening of the material is caused by these shear-cracks leading to larger shear strains. However, these shear-cracks will not lead to final fracture because the superimposed compression loading leads to contact of the crack areas which are pressed together and, therefore, relative movement is stopped for a while.

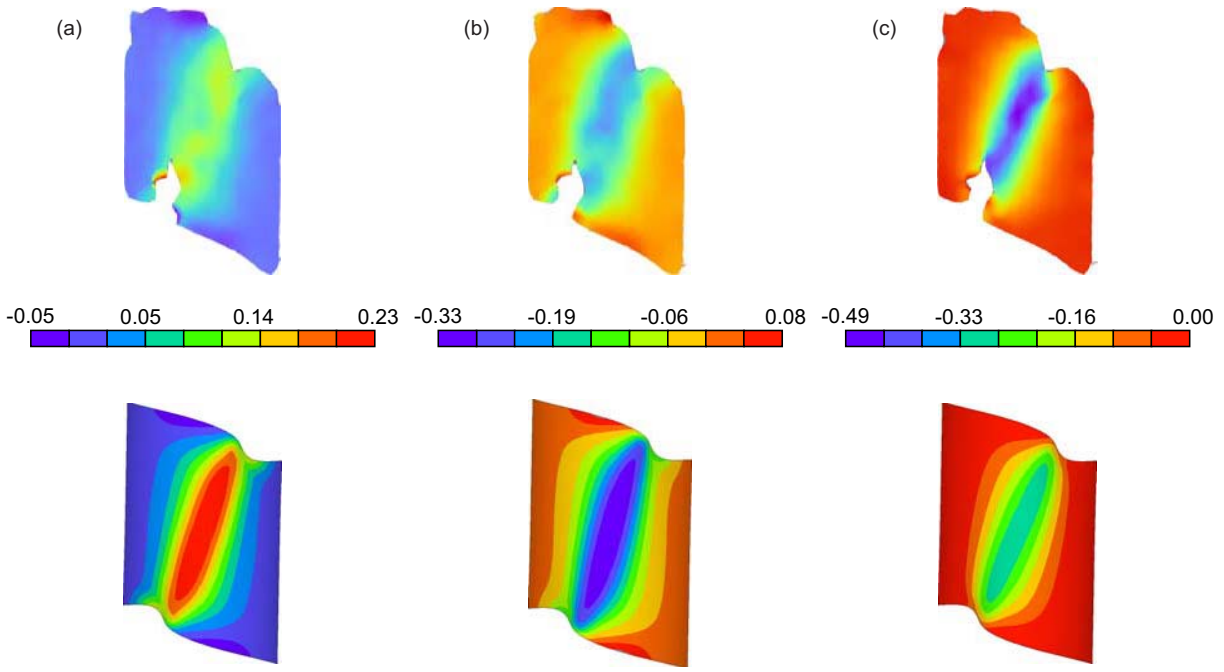

Fig. 6. Strain fields taken from DIC (top) and numerical simulation (bottom): (a) Normal strain in direction 1, (b) Normal strain in direction 2, (c) Shear strain.

This behavior cannot be simulated by the proposed approach because discontinuities cannot be taken into account in continuum models.

4. Conclusions

In the paper an anisotropic continuum damage and failure model for ductile metals has been discussed. The phenomenological approach takes into account damage tensors introduced via kinematic definition and considers the effect of stress state on damage conditions and damage strain evolution laws. Based on experimental observations as well as on numerical simulations on the macro- and micro-level different branches of these criteria have been proposed corresponding to different microscopic damage and fracture mechanisms depending on stress intensity, stress triaxiality and the Lode parameter. Stress-state-dependent damage mode functions have been developed which are able to simulate all relevant effects observed in various experiments and are suitable for practical applications.

Experiments with biaxially loaded specimens have been performed. To analyze current strain fields forming in critical regions of the specimen during loading digital image correlation technique has been used. In the present paper, the focus was on specimens loaded in the shear-compression range.

In addition, corresponding numerical simulations based on the proposed phenomenological continuum model have been performed. Detailed information on load-deformation behavior as well as on stress and strain states have been obtained. Numerical results have been compared with available experimental data especially in the critical regions of the specimen where localization of inelastic deformations and ductile fracture are expected to occur. The results of the presented experimental-numerical procedure allow validation of the proposed stress-state-dependent constitutive equations especially in the range of moderate negative stress triaxialities. Under shear-compression loading conditions it is supposed that shear-cracks occur in the center of the specimen but their areas come into contact and are pressed together. As a consequence, the activity of these cracks will be interrupted for a while but they are still existent. This behavior plays an important role for later use of formed products and can lead to remarkable reduction in their safety and lifetime. This effect will be studied in more detail by the authors in near future.

For example, the proposed phenomenological approach can be used in numerical analyses for optimization of metal forming processes. It has been shown that the macro-cracks are initiated in regions of moderate equivalent damage strains and run through bands of maximum equivalent damage strains which might give reference to propose alternative fracture criteria as a function of damage strain measures.

References

Bai Y, Wierzbicki T (2008) A new model of metal plasticity and fracture with pressure and Lode dependence. International Journal of Plasticity 24:1071–1096

Bao Y, Wierzbicki T (2004) On the fracture locus in the equivalent strain and stress triaxiality space. International Journal of Mechanical Sciences 46:81–98

Brünig M (2003) An anisotropic ductile damage model based on irreversible thermodynamics. International Journal of Plasticity 19:1679–1713

Brünig M, Chyra O, Albrecht D, Driemeier L, Alves M (2008) A ductile damage criterion at various stress triaxialities. International Journal of Plasticity 24:1731–1755

Brünig M, Gerke S, Hagenbrock V (2013) Micro-mechanical studies on the effect of the stress triaxiality and the Lode parameter on ductile damage. International Journal of Plasticity 50:49–65

Brünig M, Brenner D, Gerke S (2015) Stress state dependence of ductile damage and fracture behavior: Experiments and numerical simulations. Engineering Fracture Mechanics 141:152–169

Brünig M, Gerke S, Schmidt M (2016) Biaxial experiments and phenomenological modeling of stress-state-dependent ductile damage and fracture. International Journal of Fracture, doi: 10.1007/s10704-016-0080-3

Driemeier L, Brünig M, Micheli G, Alves M (2010) Experiments on stress-triaxiality dependence of material behavior of aluminum alloys. Mechanics of Materials 42:207–217

Dunand M, Mohr D (2011) On the predictive capabilities of the shear modified Gurson and the modified Mohr-Coulomb fracture models over a wide range of stress triaxialities and Lode angles. Journal of the Mechanics and Physics of Solids 59:1374–1394

Gao X, Zhang G, Roe C (2010) A study on the effect of the stress state on ductile fracture. International Journal of Damage Mechanics 19:75–94